Vision Res. Vol. 23, No. 9, pp. 873–882, 1983
Printed in Great Britain.

0042-6989/83 $3.00 + 0.00

SPATIAL FREQUENCY TUNING OF ORIENTATION SELECTIVE UNITS ESTIMATED BY OBLIQUE MASKING*

HUGH R. WILSON, DAVID K. MCFARLANE and GREGORY C. PHILLIPS
Department of Biophysics and Theoretical Biology, University of Chicago, 920 E. 58th Street, Chicago, IL 60637, U.S.A.

(*Received* 25 *May* 1982; *in revised form* 8 *November* 1982)

Abstract—Threshold elevations were measured as a function of the spatial frequency of high contrast cosine masks using spatially localized test stimuli with a 1.0 octave bandwidth. The cosine masks were oriented at 14.5° relative to the vertical test patterns in order to average out spatial phase effects. The experiment was repeated for each of 14 test frequencies spanning the range 0.25–22.0 c/deg in 0.5 octave steps. The resulting threshold elevation curves fell into a small number of distinct groups, suggesting the existence of discrete spatial frequency mechanisms in human central vision. The data are shown to be consistent with a model having just six distinct classes of spatial frequency mechanisms in the fovea. Spatial frequency bandwidths of these mechanisms ranged from 2.5 octaves at low frequencies to as narrow as 1.25 octaves at high spatial frequencies. These results require revision of the Wilson and Bergen (1979) [*Vision Res.* **19**, 19–32] model for spatial vision.

Spatial frequency Orientation Masking Nonlinearities Bandwidths

INTRODUCTION

The spatial frequency tuning of human visual mechanisms has generally been estimated using one of two experimental paradigms. In subthreshold summation studies the threshold for a spatial test pattern has been compared with its threshold when superimposed on a second subthreshold pattern. Using this procedure and a variety of both periodic and aperiodic patterns, spatial frequency bandwidths have been estimated to lie between about 1.0 and 1.75 octave (Mostafavi and Sakrison, 1976; Quick *et al.*, 1978; Wilson, 1978; Graham and Rogowitz, 1976; Watson, 1982). (All bandwidth measurements reported in this paper refer to the full bandwidth at half height.) All of these studies compensated for the effects of spatial probability summation, which has been shown to produce an artificial narrowing of bandwidth estimates (Stromeyer and Klein, 1975; King-Smith and Kulikowski, 1975; Graham and Rogowitz, 1976). A difficulty with all subthreshold summation studies, however, is the relatively small size of the measured effects. Thus, it is possible that discrepancies among bandwidth estimates result from inaccuracies inherent in the subthreshold summation paradigm.

Masking experiments constitute the second major method of bandwidth estimation (Stromeyer and Julesz, 1972; Legge, 1978; Legge and Foley, 1980). In contrast to subthreshold summation, masking effects are often quite large, with masked thresholds being as much as a factor of 5.0–10.0 greater than unmasked thresholds. We have therefore chosen to use a masking paradigm to estimate spatial frequency bandwidths of human visual mechanisms.

The masking experiments reported here differ from previous studies in three major respects. First, the test stimulus was spatially localized and had a bandpass Fourier transform with a full bandwidth at half height of 1.0 octave. Thus, the test patterns would be optimal stimuli for the most sharply tuned mechanisms estimated from subthreshold summation experiments. In addition, the limited spatial extent of the patterns should minimize effects due to the spatial inhomogeneity of the visual system. Second, masking functions were measured for fourteen different spatial frequencies of test patterns spanning the range 0.25–22.0 c/deg in 0.5 octave intervals. Finally, our method is novel in that the masks were oriented at 14.5° relative to the vertical test pattern (hence the name "oblique masking"). Theoretical considerations indicate that this should minimize contamination of the data either by spatial probability summation or by spatial phase effects (see Methods). In a second series of masking experiments we have verified that these oblique masks are within the orientation half-bandwidth of visual mechanisms tuned to vertical stimuli (Phillips and Wilson, 1982).

METHODS

Spatial patterns were generated by a Digital Equipment Corporation PDP/8 computer, passed through a D/A converter and displayed on a Tektronix 608 Monitor (P31 phosphor). Each pattern was one-dimensional and was defined by a list of 512 luminance values. The display, which had a mean luminance of 17.5 cd/m^2, was viewed through a circular hole in a cardboard mask that was illuminated at the

*This research was first reported at the annual meeting of the Association for Research in Vision and Ophthalmology in May, 1982.

same mean level and approximately the same hue as the monitor.

All of the masking patterns used in this study were cosine gratings, which were fixed at 40% contrast for the majority of measurements. The test stimuli had a luminance profile defined by the sixth derivative of a spatial Gaussian function and will be termed D6 patterns

$$D6(\sigma) \equiv \frac{-d^6 \exp^{-x^2/\sigma^2}}{dx^6} \quad (1)$$

where σ is the space constant in degrees of visual angle. The differentiation in equation (1) may be carried out with the result

$$D6(\sigma) = \frac{1}{\sigma^6}\left[120 - 720\left(\frac{x}{\sigma}\right)^2 + 480\left(\frac{x}{\sigma}\right)^4 - 64\left(\frac{x}{\sigma}\right)^6\right]\exp^{-x^2/\sigma^2}. \quad (2)$$

The right side of this equation is just a Gaussian multiplied by a Hermite polynomial. The Fourier transform of a D6 pattern is easily shown to be given by

$$\mathcal{F}(D6) = \sqrt{\pi}\sigma(2\pi\omega)^6 \exp^{(-\pi^2\sigma^2\omega^2)} \quad (3)$$

where ω is the spatial frequency in c/deg. From equation (3) the peak spatial frequency of a D6 may be shown to be

$$\omega_{max} = \frac{\sqrt{3}}{\pi\sigma}. \quad (4)$$

D6 patterns were chosen for this study because they are spatially localized, thus minimizing effects due to the spatial inhomogeneity of the visual system; and because they have a relatively narrow spatial frequency bandwidth of 1.0 octave. A plot of a D6 stimulus is shown in Fig. 1. A discussion of the mathematical properties of the class of Gaussian derivative stimuli may be found elsewhere (Swanson *et al.*, 1982).

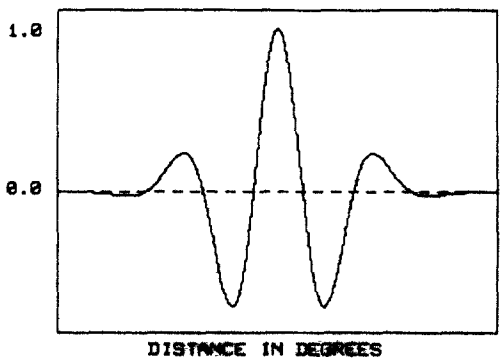

Fig. 1. Luminance profile of the test stimulus used in these experiments. The pattern is the sixth spatial derivative of a Gaussian and has a Fourier transform with a full bandwidth at half height of 1.0 octaves.

At the two lowest spatial frequencies tested, 0.25 and 0.35 c/deg, a D6 pattern was too broad to fit on the monitor. For these two frequencies, therefore, a difference of spatial Gaussian functions (DOG) was used as the test stimulus

$$DOG(\sigma) = 3\exp^{(-x^2/\sigma^2)} - 2\exp^{[-x^2/(1.5\sigma)^2]}. \quad (5)$$

In a control experiment masking functions were obtained with a 0.5 c/deg test stimulus using both a DOG and a D6 pattern. As the threshold elevation curves obtained with the two patterns were not significantly different, the use of DOGs at 0.25 and 0.35 c/deg should not be a source of error.

The oblique masking paradigm requires that the vertical test stimulus be masked by a cosine grating presented at an angle different from the vertical. This was accomplished by the use of an electronic raster rotator. The computer alternately read out the test pattern with the raster vertically oriented and the mask with the raster rotated to the desired non-vertical orientation. As 60 frames of the test were alternated with 60 frames of the mask each second, the two appeared to be physically superimposed without any visible flicker due to the frame rate.

The oblique masking results reported here were obtained with the mask oriented at 14.5° relative to the vertical test. The 14.5° mask angle was governed by several considerations. First, oblique masking studies conducted as a function of mask angle indicate that this angle is within the orientation half-bandwidth of visual mechanisms tuned to the vertical (Phillips and Wilson, 1982; Campbell and Kulikowski, 1966). Second, the use of obliquely oriented masks is dictated by the desire to have all possible spatial phase relationships between test and mask simultaneously present. This should minimize any spatial phase effects and any masking analog of spatial probability summation. (Control experiments have also shown our masking data to be independent of the spatial phase of the mask at the center of the screen.) Specifically, it can be proved that for any positive value of Q the value of the expression

$$\left\{\int_{-L}^{L}\int_{-L}^{L}\left|F(x) + \cos 2\pi w_m (x\cos\theta - y\sin\theta)\right|^Q dy\,dx\right\}^{1/Q}$$

is independent of w_m and θ as long as $2Lw_m\sin(\theta)$ is a positive integer. (We have verified experimentally that our use of a circular rather than a square field and of frequencies such as 2.83 rather than 3.0 c/deg does not affect our results.) As this integral is the appropriate two-dimensional generalization of spatial probability summation (Quick, 1974), it follows that any aspect of masking which is a function of this integral will be constant for all masks and thus can play no role in determining the *shape* of the masking function. This is particularly important, as Legge and

Foley (1980) have shown that when mask and test are at the same orientation, the degree of spatial pooling (probability summation) varies with mask strength. The choice of a 14.5° mask orientation was made so that $2Lw_m\sin(\theta)$ will be a positive integer for spatial frequencies down to 1.0 c/deg for a 4.0° diameter test field. For lower spatial frequencies an 8.0° field was used to satisfy the condition down to 0.5 c/deg. For the two lowest spatial frequencies, 0.25 and 0.35 c/deg, control experiments using a 30.0° mask angle yielded results similar to the 14.5° mask angle and we have therefore standardized on 14.5°.

The masking gratings in our experiments were temporally modulated by a 1.0 Hz sine wave. As the individual trials were of 1 sec duration, the mask passed through 1 cycle beginning at zero phase. During each 1 sec trial, the test stimulus was modulated by a Gaussian temporal waveform with a time constant of 0.25 sec (1/e to 1/e width of 0.5 sec). As the test pattern contrast peaked half way through the presentation interval, it was 90.0° out of phase with the mask. Control experiments in which both test and mask received Gaussian temporal modulation produced very similar threshold elevations, but this procedure resulted in larger standard deviations and was reported by subjects to be more difficult. Using orthogonal masks, Burbeck and Kelly (1981) also found that a 90.0° temporal phase shift between test and mask produced the same threshold elevations as the in-phase condition.

Subjects sat facing the display with their heads comfortably positioned in a chin rest. Viewing was monocular with natural pupil and the other eye was covered with a translucent occluder. They were instructed to fixate the center of the circular field, which was 4.0° in diameter for frequencies of 1.0 c/deg and above and 8.0° in diameter for lower frequencies. No fixation mark was used. The subject initiated each trial by pressing a button, which triggered a 1 sec stimulus presentation. A soft tone signalled the end of the presentation, after which the subject pressed the appropriate button to indicate whether or not they had seen the test. Based on this response the computer modified the test contrast for the next presentation using a modified version of the randomized double staircase technique described by Cornsweet (1962). Details of this technique may be found elsewhere (Wilson, 1978).

In a single experiment, thresholds were measured for a single test pattern of fixed spatial frequency, which was either superimposed on a uniform background (unmasked condition) or else on one of seven different masks. The seven mask spatial frequencies ranged from 1.5 octaves below to 1.5 octaves above the test spatial frequency in 0.5 octave steps. As no mask or test frequencies outside the range 0.25–22.0 c/deg were used, however, the lowest test frequencies were paired with masks of the seven lowest frequencies: while the highest test frequencies were paired with the seven highest mask frequencies. In each experiment the seven masks plus the unmasked condition were presented in random order.

Fourteen experiments were run on each subject for test spatial frequencies spanning the range 0.25–22.0 c/deg in 0.5 octave steps. The test frequencies for successive experiments were chosen randomly with the constraint that test frequencies 0.5 octaves apart were never used sequentially. Auxiliary experiments in which the dependence of test threshold on mask contrast was measured were also run on all subjects. The three subjects from whom complete data sets were obtained included two of the authors plus a naive observer, who had no training in psychophysics and no knowledge of the purpose of these experiments. Partial data sets were also obtained on two further naive observers.

RESULTS

The purpose of these experiments was to estimate the spatial frequency tuning of human visual mechanisms. In a separate series of masking experiments it was verified that the mechanisms revealed by oblique masking are orientation selective and that the mask orientation of 14.5° falls within their half amplitude half bandwidth (Phillips and Wilson, 1982).

As we felt it important to determine whether oblique masking might be due to some form of lateral interaction between test and mask, such as inhibition, we performed a control experiment in which the mask was present on either side of the stimulus but did not overlap it. As the resulting data showed no evidence of masking, we conclude that oblique masking is not due to lateral interactions.

Oblique masking curves were obtained using each of fourteen test frequencies between 0.25 and 22.0 c/deg in 0.5 octave steps. Adjacent spatial frequencies were never run in successive experiments and were thus always run on different days. When data collection was completed and threshold elevation curves compared, we discovered that neighboring test frequencies often produced very similar threshold elevation curves. As an example, consider the three data sets in Fig. 2, which were obtained with test frequencies of 0.35 (open circles), 0.50 (solid circles) and 0.71 c/deg (open squares). In this and all subsequent graphs the threshold elevation is defined as the ratio of masked to unmasked test threshold contrast, so a value of 1.0 indicates that no masking occurred. For both subjects the data fall within experimental error of defining a single curve. In addition, peak masking is obtained for a mask spatial frequency between 0.7 and 1.0 c/deg, which is significantly above the two lower test frequencies. As data obtained at 0.25 c/deg superimpose on those shown (they are omitted for clarity), this suggests that the largest spatial mechanisms processing foveal information have a peak spatial frequency tuning of

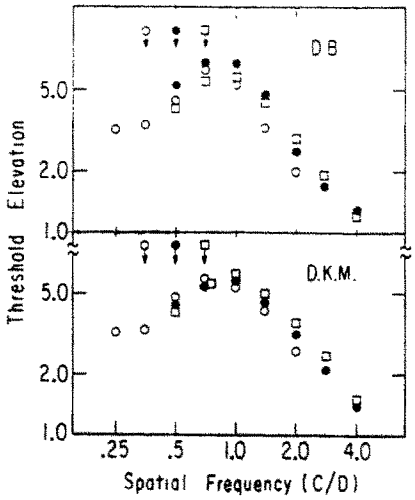

Fig. 2. Oblique masking functions obtained with test frequencies of 0.35 (open circles), 0.50 (solid circles), and 0.71 (open squares) c/deg. For each subject the three threshold elevation curves are very similar and peak between 0.7 and 1.0 c/deg regardless of the spatial frequency of the test stimulus. These data suggest that the lowest spatial frequency mechanisms in central vision are tuned to about 0.75 c/deg.

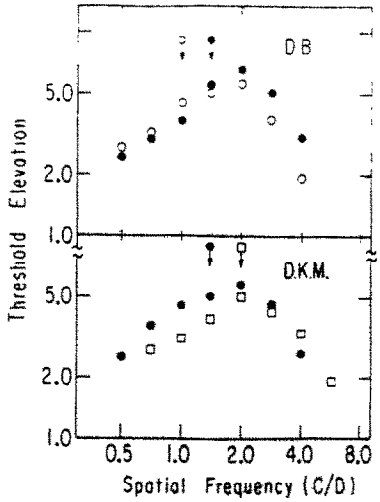

Fig. 3. Threshold elevation curves for two intermediate test frequencies. For D.B. these were 1.0 (open circles) and 1.4 (solid circles) c/deg, and for D.K.M. they were 1.4 (solid circles) and 2.0 (open squares) c/deg. For each subject the two curves are similar in shape and peak at 2.0 c/deg, suggesting that the two test patterns are detected by a single visual mechanism.

about 0.7–1.0 c/deg. The same pattern was evident in data obtained from a third subject.

Figures 3 and 4 compare data obtained at intermediate and higher test spatial frequencies respectively. In Fig. 3 the two data sets on each subject peak at 2.0 c/deg and have very nearly the same shape. Note that the two curves for D.B. were obtained with test frequencies of 1.0 and 1.4 c/deg, while those for D.K.M. were obtained with test frequencies of 1.4 and 2.0 c/deg. Individual differences of this nature were found in several instances, and these differences are reflected in our data analysis (see Fig. 10). Figure 4 compares threshold elevation curves measured with test frequencies of 8.0 and 11.3 c/deg. Again, the two curves for each subject are very similar. In contrast to the low frequency data in Fig. 2, the most effective masks for high frequency test patterns tend to occur at mask frequencies lower than the test.

To determine the statistical significance of the grouping of threshold elevation curves evident in Figs 2–4, the correlation coefficients between curves within a group were calculated and compared with the correlation between curves obtained with neighboring test frequencies but not falling into the same grouping. For subject D.B. for example, the correlations between curves obtained with test frequencies of 0.35 and 0.7, 0.5 and 0.7 and 0.7 and 1.0 c/deg were 0.935, 0.986 and 0.495 respectively. Using Fisher's r-to-z transformation, it was found that the first two values were not significantly different; but both were significantly different from the third value ($P < 0.01$). Thus, we conclude that the grouping in Fig. 2 is statistically significant. Similar results were obtained for the other groupings shown and for data on a third subject.

The major qualitative features of our masking data may be summarized as follows. First, the most effective masks for low spatial frequency test patterns tend to be of higher spatial frequency than the test. This result was also found by Legge and Foley (1980) using spatially localized test stimuli. Second, the most effective masks for high spatial frequency test patterns tend to be of lower spatial frequency than the test. Third, threshold elevation curves obtained with neighboring test spatial frequencies are often very highly correlated with one another.

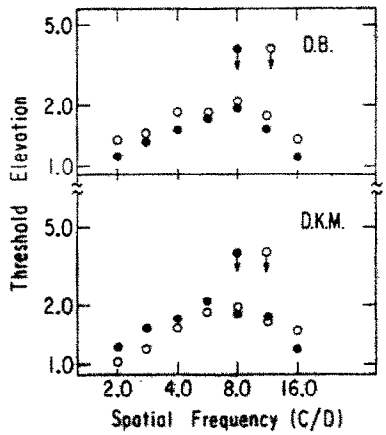

Fig. 4. Oblique masking curves for test frequencies of 8.0 (solid circles) and 11.3 (open circles) c/deg. The similarity of the two data sets for each subject suggests that a single spatial frequency tuned mechanism with a peak sensitivity of about 8.0 c/deg is detecting both test patterns.

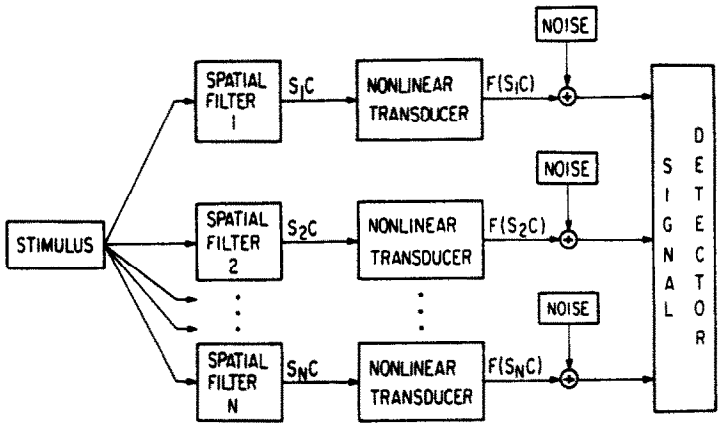

Fig. 5. Schema of the masking model used to analyze the oblique masking data. The test stimulus plus mask are processed in parallel by several linear spatial filters with differing tuning curves. The output of this stage is therefore a product of stimulus contrast C and filter sensitivity S. Signals are subsequently passed through empirically characterized nonlinearities and noise is then added. Finally, a signal detector decides whether the noisy signal was due to the mask alone or to mask plus test.

DATA ANALYSIS

In this section the spatial frequency tuning characteristics of the visual mechanisms underlying oblique masking will be estimated on the basis of a very simple visual model. The elements of this model are diagrammed in Fig. 5. The stimulus is first processed in parallel by a number of linear spatial frequency filters. The output of each filter is then passed through a nonlinearity, the characteristics of which may differ from filter to filter. Following this, noise (uncorrelated from filter to filter) is added to each response, and the resultant noisy signals then provide the input to a signal detector. As masking is basically an increment threshold task, the role of the signal detector is to determine whether the response to the test pattern plus mask is significally different from the response that would have been generated by the mask alone. This model is essentially the same as those used in several previous studies to analyze masking and increment threshold data (Carlson, 1978; Carlson and Cohen, 1980; Legge and Foley, 1980; Wilson, 1980a).

In order to employ this model, it is necessary to measure the characteristics of the nonlinear stage. This can be done by determining the dependence of threshold elevation on oblique mask contrast. We have conducted these experiments at test spatial frequencies of 0.5, 2.0, 4.0 and 11.3 c/deg using mask contrasts of 5, 10, 20 and 40%. In each case the mask frequency was identical to that of the test. Results showing threshold elevation as a function of mask contrast for three subjects are plotted in Fig. 6. In all cases the data are well fit by a straight line in log–log coordinates, thus implying a power law relationship between mask contrast and threshold elevation. As the data for all subjects at a single spatial frequency had very similar slopes, a single least mean squares fit was made to the data at each spatial frequency. For the lowest three frequencies, the resulting power law exponent was approximately constant at 0.55, which is close to the value of 0.60 found by Legge (1981) at 2.0 c/deg. At 11.3 c/deg, however, the slope of the data is obviously significantly shallower, leading to an estimated exponent of 0.24.

The data in Figure 6 indicate that the dependence of threshold elevation on contrast can be described by a function of the form

$$\Delta C = \max\left\{C_{\text{th}}, \frac{H}{S_T}(S_M C_M)^{\epsilon}\right\}. \tag{6}$$

This function is identical to the threshold contrast, C_{th}, until a mask contrast is reached at which the

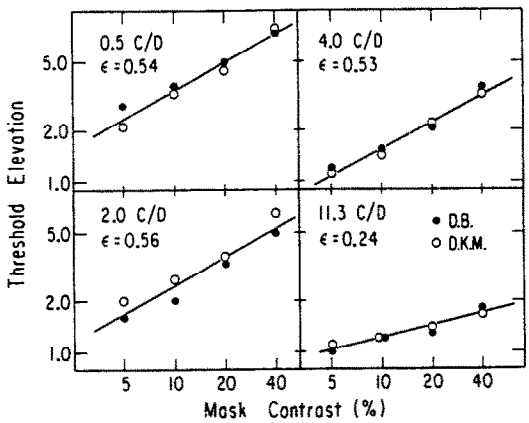

Fig. 6. Dependence of threshold elevation on mask contrast for spatial frequencies of 0.5, 2.0, 4.0 and 11.3 c/deg. For both subjects and all spatial frequencies the relationship is well described by a straight line on log–log coordinates, thus indicating a power law. The power law exponent is approximately constant at about 0.55 for low and intermediate frequencies, but it decreases to about 0.25 at 11.3 c/deg.

increment threshold produced by a power law becomes greater than the threshold contrast. Although this relationship does not incorporate the dip in increment thresholds for mask contrasts near threshold as documented by Nachmias and Sansbury (1974), the 40% mask contrast used in the main body of our experiments was always far above threshold. Equation (6), with exponents from Fig. 6 and the values of H estimated from individual subject's data provides a complete empirical characterization of the nonlinear and noise addition stages of the model in Fig. 5. (Note that the data in Fig. 6 actually provide an estimate of the nonlinear dependence of the signal to noise ratio on contrast.)

Finally, it is necessary to specify the manner in which the incremental responses of the different spatial mechanisms are to be combined in the signal detection stage. Here we take our cue from studies of threshold spatial vision, which commonly assume that responses of independent mechanisms should be combined according to probability summation (King-Smith and Kulikowski, 1975; Graham and Rogowitz, 1976; Stromeyer and Klein, 1975; Wilson and Bergen, 1979). Adopting the Quick (1974) formulation for inter-mechanism probability summation with an exponent of 4.0 (all values above about 3.0 produce very similar results), the masked threshold contrast ΔC is given in terms of the increment thresholds for the individual mechanisms ΔC_i by the formula

$$\frac{1}{\Delta C} = \left[\sum_{i=1}^{N} \frac{1}{\Delta C_i^4} \right]^{1/4}. \quad (7)$$

Note that this equation is written in terms of the reciprocals of the individual mechanism responses, as probability summation combines sensitivities rather than contrasts.

Given equations (6) and (7), there remains only the task of estimating the number of mechanisms and their spatial frequency filter characteristics from the oblique masking data. As both equations are highly nonlinear, this was done using a two stage, self-consistent iterative routine. In the first stage data sets for individual test frequencies were read in one at a time. For each new data set the computer first attempted to compute the unmasked sensitivity of that mechanism N to the test pattern, $S_N(T)$, according to the rearrangement of equation (7)

$$S_N(T) = \left[F^4 - \sum_{i=1}^{N-1} S_i^4(T) \right]^{1/4}. \quad (8)$$

This equation simply requires that the fourth norm of the individual mechanism sensitivities to the test pattern in question equal the empirically determined threshold sensitivity F. Following this, the program then attempted to estimate the value of the parameter H [see equation (6)] for that mechanism from the data point obtained with test and mask of the same spatial frequency. This was done by first computing the incremental contrast response for mechanism N from equation (7) and then using this in equation (6). Given the values of H and $S_N(T)$ for the new mechanism, it is then possible to use equations (6) and (7) to determine this mechanism's sensitivity to each of the other masking gratings from the measured value of the masked threshold.

The procedure just outlined guarantees that each new mechanism introduced will be consistent with the responses of all mechanisms that have been previously calculated. In addition, the procedure provides an inherent constraint on the number of mechanisms. Note that if the term in brackets in equation (8) is negative, then it is impossible to compute a real value for the sensitivity for the new mechanism. In this case the computer indicated that the new data set could not be used to compute a new mechanism. The interpretation of this constraint is quite simple: if the mechanisms previously computed already fit the threshold sensitivity of the new test pattern, then no new mechanism can be involved in determining that sensitivity. Thus, this model requires that *each visual mechanism must be more sensitive than any other mechanism to at least one test frequency*. This assumption not only seems to be implicit in all current models of spatial vision but also is necessary in order to avoid an unlimited number of degrees of freedom in the data analysis.

Using this program with the fourteen sets of oblique masking data for each subject, it was found that distinct mechanisms could only be computed from six sets for each subject. There were two reasons for this. First, the clustering of neighboring data sets shown in Figs 4–6 resulted in essentially identical mechanisms being calculated based on any one of the curves. Second, the sensitivities computed from a given data set were often such that they accounted for the threshold sensitivities for one or more neighboring test patterns and in this case, the computer could not compute mechanisms from the neighboring data sets for the reasons discussed above. At this point, the six mechanisms estimated from the initial analysis were input to a second program. This program generated predicted threshold elevation curves for all data sets and then varied the individual mechanism sensitivities in small increments so as to maximize the percentage of the variance accounted for by the model. The resulting fits to the data for two of the subjects are shown in Figs 7 and 8. For each subject the six mechanism fit accounted for 93% of the variance. The error bars shown on one data point in each figure are typical and indicate that in the worst cases the six mechanism fit deviates from the data by about one standard deviation. Figure 9 shows that the six computed mechanisms simultaneously provided a good fit to the unmasked threshold sensitivities for the D6 test patterns.

The mechanisms estimated from the data for each of three subjects are shown in Fig. 10. The solid curves are drawn through the geometric means of the data in each panel. For comparison, the four dashed

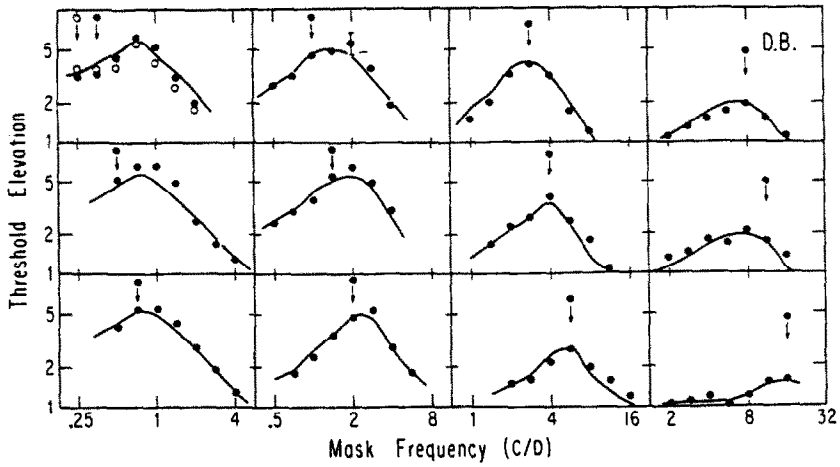

Fig. 7. Comparison of oblique masking data for D.B. with the predictions of a six mechanism model that was fit to the data. Test frequencies begin with 0.25 and 0.35 c/deg in the upper left box and progress downward and to the right in 0.5 octave steps, ending with 16.0 c/deg in the lower right bow. The six mechanisms estimated from the data account for 93% of the variance. The error bars indicate the standard deviation typical of these data. Note that the spatial frequency scale has been progressively shifted to higher frequencies for successive columns.

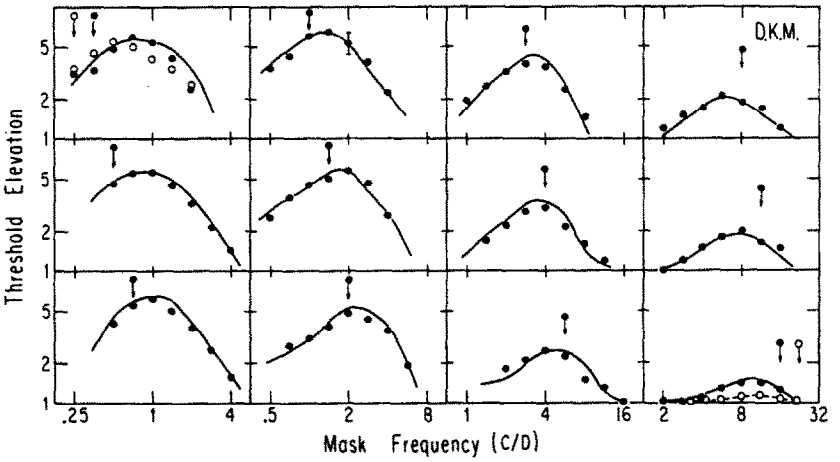

Fig. 8. Fit of a six mechanism masking model to the oblique masking data for D.K.M. The six mechanisms account for 93% of the variance. All details are the same as for Fig. 9, except that data for a test frequency of 22.0 c/deg have been included in the lower right box.

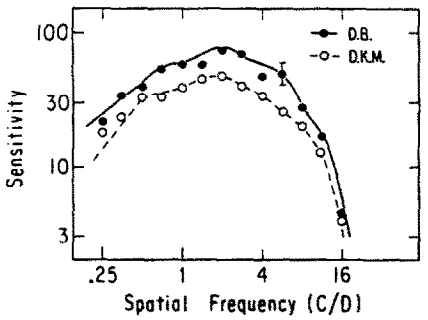

Fig. 9. Fit of the six mechanisms derived from masking data to the unmasked test sensitivities. The masking model required that the filters simultaneously fit both the masking and threshold data. Curve shapes for the two subjects were very similar, except the D.K.M. was somewhat less sensitive than D.B. Error bars indicate the standard deviation typical of these data.

curves indicate the sensitivities of the four mechanisms of the Wilson and Bergen (1979) model for threshold spatial vision. From panel A to panel F, the peaks of the solid curves occur at 0.8, 1.7, 2.8, 4.0, 8.0 and 16.0 c/deg. Although there is reasonable agreement among subjects, several individual differences are evident. For example, DB showed the steepest fall-off at high frequencies in panel A and the steepest fall-off at low frequencies in D and F.

Spatial frequency bandwidths for all mechanisms are plotted in Fig. 11 as a function of peak spatial frequency. The solid line drawn through the means of the points indicates that bandwidths are between 2.0 and 2.5 octaves at the lowest frequencies but drop to between 1.25 and 1.5 octaves at higher frequencies. For comparison, the dashed line shows the expected decline if bandwidths were constant on a linear scale.

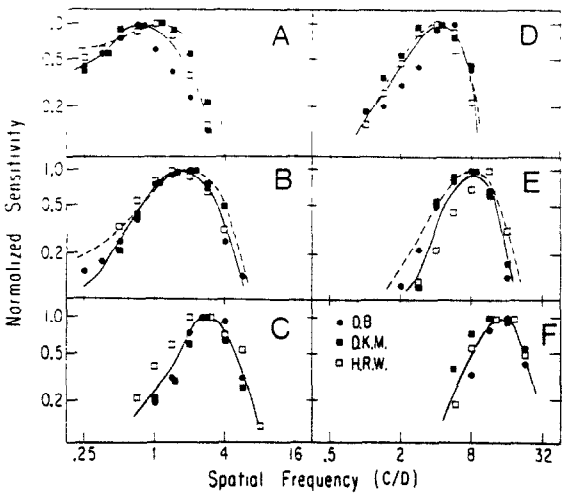

Fig. 10. Spatial frequency sensitivities of the six mechanisms fit to the oblique masking data for each of three subjects. Solid curves have been drawn through the geometric means of the points in each panel. From A–F the filters peak at 0.75, 1.5, 2.8, 4.4, 8.0 and 16.0 c/deg. All filters have been normalized to a peak value of unity. The dashed curves in A, B, D and E indicate the spatial frequency sensitivities of the four mechanisms of the Wilson and Bergen (1979) model for threshold spatial vision.

This would be expected if the visual system performed a two-dimensional Fourier analysis on patches of the visual image.

One final point should be emphasized in connection with the data analysis in Figs 10 and 11. The grouping of threshold elevation curves in Figs 2–4 provides evidence for the existence of discrete mechanisms at both low and high spatial frequencies. However, our data do not permit us to discriminate between two discrete mechanisms and a continuum in the frequency range from about 2.5 to 5.0 c/deg.

DISCUSSION

Threshold elevations obtained with grating masks oriented at 14.5° relative to the vertical test pattern provide evidence for discrete spatial frequency tuned mechanisms at both low and high spatial frequencies. This evidence derives from the fact that test stimuli differing in peak spatial frequency by 0.5 octaves or more produce highly correlated threshold elevation curves. In consequence, peak masking often occurs for mask frequencies that differ from the test frequency. Comparable data at low spatial frequencies have also been reported by Legge (1978, 1979). For test frequencies in the range 2.5–5.0 c/deg, however, the data are compatible either with discrete mechanisms or with a continuum. It is likely that previous masking studies have failed to find evidence for discrete mechanisms at high and low frequencies for either of two reasons. First, previous studies have not measured threshold elevation curves for closely spaced test spatial frequencies throughout most of the visible range. Without such evidence it would be impossible to determine whether threshold elevation curves fell into a small number of groups. Second, most previous masking studies have used cosine gratings rather than spatially localized test patterns. Thus, the variation of visual properties with eccentricity may have served to obscure evidence for discrete mechanisms in central vision. Here it may be noted that Legge and Foley (1980) obtained data similar to ours when masking spatially localized test patterns with gratings but not when masking gratings with gratings. In addition, adaptation to cosine gratings provides evidence for the existence of discrete mechanisms when spatially localized test patterns are used (Williams *et al.*, 1982) but not when testing is done with cosine gratings (Blakemore and Campbell, 1969).

Recently, Stromeyer *et al.* (1982) have presented evidence suggesting that there are visual mechanisms tuned to very low spatial frequencies. This is at odds with our low frequency data (Fig. 2) and with masking data obtained by Legge (1978, 1979). However, Stromeyer *et al.* (1982) used cosine test gratings up to 18.0° wide. Recent estimates of the variation of receptive field size with eccentricity in both cats (Cleland *et al.*, 1979) and humans (Wilson and Bergen, 1979) indicate that fields at 9.0° eccentricity are about 2.5 times wider than fields at fixation. Thus, the very low frequency units reported by Stromeyer *et al.* (1982) may well be located eccentrically. Blakemore and Campbell (1969) also failed to find evidence for very low frequency units when using small field gratings.

From an analysis of oblique masking data on three subjects, it has been shown that six bandpass spatial frequency filters provide an excellent fit to the data. Although individual differences have been noted, intersubject agreement is generally good. The bandwidths are between 2.0 and 2.5 octaves for the two lowest frequency mechanisms but from 1.25 to 1.5

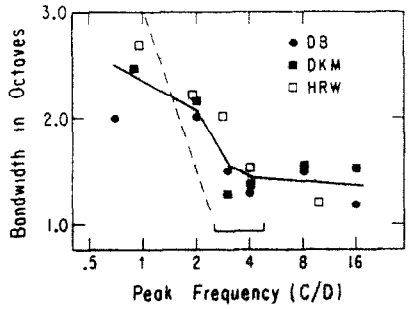

Fig. 11. Spatial frequency bandwidths of visual mechanisms for three subjects as a function of peak spatial frequency. The solid line is drawn through the mean values. The dashed line indicates how bandwidths would be expected to vary if the visual system performed a Fourier analysis on patches of the retinal image. The bracket from 2.5 to 5.0 c/deg indicates the region within which it is not possible to distinguish between discrete mechanisms and a small continuum.

octaves for intermediate and high frequencies (see Fig. 13). This is in reasonable agreement with previous masking studies (Stromeyer and Julesz, 1972; Legge, 1978; Legge, 1979; Legge and Foley, 1980). Physiological measurements of the spatial frequency tuning of cat cortical cells have also shown that the mean bandwidth is 1.5 octaves, with few cells falling outside the range 1.0–2.5 octaves (Movshon *et al.*, 1978a). In agreement with both psychophysics (Rentschler and Hilz, 1976; Blakemore and Campbell, 1969) and cortical physiology (Movshon *et al.*, 1978b) the receptive fields for the narrower bandwidth mechanisms show a central excitatory zone flanked by inhibitory zones which are in turn flanked by small secondary excitatory zones.

As our masks were oriented at 14.5° relative to the test patterns, it is important to determine whether our mechanism sensitivity profiles and bandwidths need to be corrected for mask orientation. Phillips and Wilson (1982) have attempted to determine whether two-dimensional visual filters are separable in either Cartesian or polar coordinates. Results for a wide range of orientations indicate that these filters have characteristics that fall between the predictions of Cartesian and polar separability (see also Daugman, 1980, 1982). For orientations out to about 20.0°, however, human visual filters are well approximated by a product of spatial frequency and orientation functions (polar separability). Thus, oblique masking should accurately reflect the spatial frequency tuning characteristics of these filters.

An examination of our results in light of the sustained-transient dichotomy merits brief mention. Preliminary experiments in which oblique masking was measured as a function of the temporal frequency of the mask suggest that the two lowest frequency mechanisms in the present study have transient temporal characteristics, while the remaining four are sustained. This agrees with orthogonal masking results in which mechanisms tuned to frequencies below about 2.0 c/deg were found to have transient characteristics (Burbeck and Kelly, 1981). The spatial frequency tuning characteristics of a low frequency transient mechanism have been independently estimated using both masking (Legge, 1978; Green, 1981) and subthreshold summation techniques (Wilson, 1980b). The results of all these studies are in agreement with the data in Fig. 10(A). As a further point of interest, Fig. 11 suggests that transient mechanisms have significantly wider bandwidths than sustained mechanisms. Evidence for this has also been provided by Watson and Robson (1981), Legge (1978, 1979) and Stromeyer *et al.* (1982).

Finally, the mechanisms estimated from oblique masking data may be compared with two recent models for spatial vision. On the basis of subthreshold summation data Wilson and Bergen (1979) concluded that there might be as few as four discrete mechanisms in human central vision. These mechanisms are plotted with dashed lines in Fig. 10. The reasonable agreement with the data suggests that the Wilson and Bergen (1979) model provided a good first approximation. However, that model must be modified, as we now have evidence for two additional mechanisms. Evidence for the additional highest frequency mechanism was first presented by Marr *et al.* (1980) and Watson (1982). In addition, the bandwidths obtained from oblique masking are somewhat narrower than the Wilson and Bergen (1979) estimates.

In a study of discrimination near threshold, Watson and Robson (1981) obtained evidence for seven spatial frequency mechanisms spanning the range from 0.25 to 32.0 c/deg. Although they did not estimate spatial frequency tuning characteristics from their data, the six mechanisms in Fig. 10 correspond well with six of their mechanisms. The discrepancy occurs at the lowest spatial frequencies, where Watson and Robson postulate the existence of a seventh mechanism. However, the data in our Fig. 2 provide strong evidence against the existence of a foveal mechanism with a peak frequency below about 0.75 c/deg. This apparent discrepancy between the two studies would be resolved if the lowest frequency patterns in the Watson and Robson (1981) study were discriminated on the basis of spatial information (i.e. the spatial distribution of responding units) rather than spatial frequency information.

Acknowledgements—We are indebted to J. Ennesser for building our raster rotator. This research was funded in part by NSF grant BNS-8113574 to H.R.W.

REFERENCES

Bergen J. R., Wilson H. R. and Cowan J. D. (1979) Further evidence for four mechanisms mediating vision at threshold: Sensitivities to complex gratings and aperiodic stimuli. *J. opt. Soc. Am.* **69**, 1580–1587.

Blakemore C. and Campbell F. W. (1969) On the existence of neurones in the human visual system selectively sensitive to the orientation and size of retinal images. *J. Physiol.* **203**, 237–260.

Burbeck C. A. and Kelly D. H. (1981) Contrast gain measurements and the transient/sustained dichotomy. *J. opt. Soc. Am.* **71**, 1335–1342.

Campbell F. W. and Kulikowski J. J. (1966) Orientational selectivity of the human visual system. *J. Physiol.* **187**, 437–445.

Carlson C. R. (1978) Thresholds for perceived image sharpness. *Photogr. Sci. Engng* **22**, 69–71.

Carlson C. R. and Cohen R. W. (1980) A simple psychophysical model for predicting the visibility of displayed information. *Proc. S.I.D.* **21**, 229–246.

Cleland B. G., Harding T. H. and Tulunay-Keesey U. (1979). Visual resolution and receptive field size: Examination of two kinds of cat retinal ganglion cell. *Science* **205**, 1015–1017.

Cornsweet T. N. (1962) The staircase method in psychophysics. *Am. J. Psychol.* **75**, 485–491.

Daugman J. G. (1980) Two-dimensional spectral analysis of cortical receptive field profiles. *Vision Res.* **20**, 847–856.

Daugman J. G. (1982) Polar spectral nonseparability of two-dimensional spatial frequency channels. *Invest. Opthal. visual Sci. Suppl.* **22**, 49.

DeValois R. L., Albrecht D. G. and Thorell L. G. (1982) Spatial frequency selectivity of cells in macaque visual cortex. *Vision Res.* **22**, 545–559.

Graham N. and Rogowitz B. E. (1976) Spatial pooling properties deduced from the detectability of FM and quasi-AM gratings. A reanalysis. *Vision Res.* **16**, 1021–1026.

Green M. (1981) psychophysical relationships among mechanisms sensitive to pattern, motion and flicker. *Vision Res.* **21**, 971–984.

King-Smith P. E. and Kulikowski J. J. (1975) The detection of gratings by independent activation of line detectors. *J. Physiol.* **247**, 237–271.

Legge G. E. (1978) Sustained and transient mechanisms in human vision: temporal and spatial properties. *Vision Res.* **18**, 69–82.

Legge G. E. (1979) Spatial frequency masking in human vision: binocular interactions. *J. opt. Soc. Am.* **69**, 838–847.

Legge G. E. (1981) A power law for contrast discrimination. *Vision Res.* **21**, 457–469.

Legge G. E. and Foley J. M. (1980) Contrast masking in human vision. *J. opt. Soc. Am.* **70**, 1458–1470.

Marr D., Poggio T. and Hildreth E. (1980) Smallest channel in early human vision. *J. opt. Soc. Am.* **70**, 868–870.

Mostafavi H. and Sakrison D. J. (1976) Structure and properties of a single channel in the human visual system. *Vision Res.* **16**, 957–968.

Movshon J. A., Thompson I. D. and Tolhurst D. J. (1978a) Spatial and temporal contrast sensitivity of neurones in areas 17 and 18 of the cat's visual cortex. *J. Physiol.* **283**, 101–120.

Movshon J. A., Thompson I. D. and Tolhurst D. J. (1978b) Spatial summation in the receptive fields of simple cells in the cat's striate cortex. *J. Physiol.* **283**, 53–77.

Nachmias J. and Sansbury R. V. (1974) Grating contrast: discrimination may be better than detection. *Vision Res.* **14**, 1039–1042.

Phillips G. C. and Wilson H. R. (1982) Orientation selectivity as revealed by psychophysical masking. *Invest. Ophthal. visual Sci. Suppl.* **22**, 254.

Quick R. F. (1974) A vector-magnitude model for contrast detection. *Kybernetik* **16**, 65–67.

Quick R. F., Mullins W. W. and Reichert T. A. (1978) Spatial summation effects on two component grating thresholds. *J. opt. Soc. Am.* **68**, 116–121.

Rentschler I. and Hilz R. (1976) Evidence for disinhibition in line detectors. *Vision Res.* **16**, 1299–1302.

Stromeyer C. F. and Julesz B. (1972) Spatial-frequency masking in vision: critical bands and the spread of masking. *J. opt. Soc. Am.* **62**, 1221–1232.

Stromeyer C. F. and Klein S. (1975) Evidence against narrowband spatial frequency channels in human vision: the detectability of frequency modulated gratings. *Vision Res.* **15**, 899–910.

Stromeyer C. F., Klein S., Dawson B. M. and Spillmann L. (1982) Low spatial frequency channels in human vision: Adaptation and masking. *Vision Res.* **22**, 225–234.

Swanson W. H., Wilson H. R. and Giese S. (1982) Contrast increment thresholds predict contrast matches. *Invest. Ophthal. visual Sci., Suppl.* **22**, 254.

Watson, A. B. (1982) Summation of grating patches indicates many types of detector at one retinal location. *Vision Res.* **22**, 17–26.

Watson A. B. and Robson J. G. (1981) Discrimination at threshold: Labelled detectors in human vision. *Vision Res.* **21**, 1115–1122.

Williams D. W., Wilson H. R. and Cowan J. D. (1982) Localized effects of spatial frequency adaptation. *J. opt. Soc. Am.* **72**, 878–887.

Wilson H. R. (1978) Quantitative characterization of two types of line-spread function near the fovea. *Vision Res.* **18**, 971–981.

Wilson H. R. (1980a) A transducer function for threshold and suprathreshold human vision. *Biol. Cybernet.* **38**, 171–178.

Wilson H. R. (1980b) Spatiotemporal characterization of a transient mechanism in the human visual system. *Vision Res.* **20**, 443–452.

Wilson H. R. and Bergen J. R. (1979) A four mechanism model for threshold spatial vision. *Vision Res.* **19**, 19–32.